

Lipid MALDI MS Profiling Accurately Distinguishes Papillary Thyroid Carcinoma from Normal Tissue

Junsun Ryu^{1*}, Geul Bang^{2*}, Jeong Hwa Lee^{3*}, Seung Ho Choi¹, Yuh-Seog Jung¹, Kwang Pyo Kim³, Young Hwan Kim^{2,4*} and Hark Kyun Kim^{1*}

¹National Cancer Center, Goyang, Gyeonggi, 410-769, Republic of Korea

²Division of Mass Spectrometry Research, Korea Basic Science Institute, Ochang, 363-883, Republic of Korea

³Department of Molecular Biotechnology, Konkuk University, Seoul 143-701, Republic of Korea

⁴Graduate School of Analytical Science and Technology, Chungnam National University, Daejeon, Republic of Korea

Abstract

Background: Histology-directed tissue Matrix-Assisted Laser Desorption/Ionization Mass Spectrometry (MALDI MS) has been used to identify lipid profiles that can distinguish cancerous epithelium from normal epithelium.

Methods: In order to evaluate if lipid profiles may assist with diagnosis, frozen resected tumor samples collected from papillary thyroid carcinoma patients were analyzed using Matrix (DHB/CHCA)-Assisted Laser Desorption/Ionization (MALDI) Mass Spectrometry (MS), together with adjacent normal tissue samples.

Results: Lipid peaks differentially expressed between cancer and normal samples at a feature selection $P < 0.001$ correctly predicted class labels of test set samples (7 pairs) in 100 random training-to-test partitions, at the median class prediction accuracy of 100%. In addition, lipid peaks differentially expressed between 14 pairs of cancer and adjacent normal samples correctly predicted 100% of validation set samples (8 out of 8 samples). Phosphatidylcholines (PC) 32:0 and PC 34:1, sphingomyelin 34:1, and several phosphatidylinositols were overexpressed, while lysophosphatidylcholine 18:3 and lysophosphatidylserine 18:1 were underexpressed in papillary thyroid carcinomas, compared with normal tissue.

Conclusions: Lipid MALDI MS profiles accurately distinguish papillary thyroid carcinoma epithelium from normal epithelium, and demonstrate the potential as a diagnostic aid.

Keywords: MALDI; Lipid; Papillary thyroid carcinoma

Introduction

Thyroid cancer is the most common cancer in Korea, with papillary thyroid carcinoma being the most frequent histologic subtype [1,2]. Preoperative histopathologic diagnosis is based on the degree of atypia of biopsy samples. According to the National Cancer Institute Thyroid FNA State of the Science Conference, thyroid lesions are categorized as benign, atypia, follicular neoplasm, suspicious for malignancy, and malignant [3,4]. Suspicious for malignancy category includes papillary thyroid cancers displaying subtle and focal nuclear and architectural changes [5]. Nodules called suspicious for papillary carcinoma are usually resected, and most (60–75%) prove to be papillary carcinomas [4]. Given the difficulty in diagnosing papillary thyroid carcinoma using small tissue samples, therefore, more sensitive and specific diagnostic tools are urgently needed for this disease [6].

Histology-directed Tissue Matrix-Assisted Laser Desorption/Ionization (MALDI) Mass Spectrometry (MS) is a sensitive proteomic technology that can distinguish cancerous epithelium from normal epithelium [7]. We and others have demonstrated that MALDI MS can also be used to obtain lipid profiles in clinical tissue samples [8–12]. We have previously reported that lipid profiles accurately differentiate lung cancers from normal tissue [8]. Recently, Ishikawa et al. [12] reported thyroid cancer-specific lipid MALDI MS profiles using relatively small number of thyroid cancer specimens, but they did not validate the clinical utility of this approach in sufficiently large number of patients. Using a larger set of clinical samples, here we demonstrate that lipid profiles that may possibly assist with the diagnosis of papillary thyroid carcinomas.

Materials and Methods

Tissue preparation and MALDI MS data acquisition

Samples were obtained, with informed consent and institutional review board approval, from 22 papillary thyroid cancer patients undergoing surgery at National Cancer Center in Korea. Twenty of them (90.1%) were female. Samples were collected at the time of surgery, and stored at liquid nitrogen until analysis. Thin (10 μm) cryosection slides were obtained from frozen tissues. One glass slide cryosection was stained with Hematoxylin and Eosin (H&E), and the other sections were thaw-mounted onto an Indium Tin Oxide (ITO) slide (HST Inc., Newark, NJ), desiccated in vacuum for subsequent MALDI MS profiling. The H&E-stained cryosection slide was evaluated tumor-rich (>75%) area [8–10].

We prepared the MALDI MS matrix solution by dissolving 7 mg each of 2,5-dihydroxybenzoic acid (DHB) and α -cyano-4-

***Corresponding authors:** Young Hwan Kim, Korea Basic Science Institute, 804-1 Yangcheon, Ochang, Cheongwon, Chungbuk, 363-883, Republic of Korea, Tel: +82-43-240-5140; Fax: + 82-43-240-5159; E-mail: yhkim@kbsi.re.kr

Hark Kyun Kim, Biomolecular Function Research Branch, Research Institute, National Cancer Center, 323 Ilsanro, Ilsan, Goyang, Gyeonggi, 410-769, Republic of Korea, Tel: +82-31-920-2238; Fax: +82-31-920-2006; E-mail: hkim@ncc.re.kr

Received February 15, 2013; **Accepted** April 01, 2013; **Published** April 04, 2013

Citation: Ryu J, Bang G, Lee JH, Choi SH, Jung YS, et al. (2013) Lipid MALDI MS Profiling Accurately Distinguishes Papillary Thyroid Carcinoma from Normal Tissue. J Proteomics Bioinform 6: 065-071. doi:10.4172/jpb.1000263

Copyright: © 2013 Ryu J, et al. This is an open-access article distributed under the terms of the Creative Commons Attribution License, which permits unrestricted use, distribution, and reproduction in any medium, provided the original author and source are credited.

hydroxycinnamic acid (CHCA) in 1 ml of 70% methanol plus 0.1% TFA and 1% piperidine [8] and deposited the matrix on tissue-loaded ITO slides using the CHIP-1000 instrument (Shimadzu, Kyoto, Japan). Mass spectra were acquired using UltrafleXtreme (Bruker Daltonics) at a laser frequency of 1,000 Hz. An external calibration was conducted using lipid-mixed calibration standards with m/z 674-834 (positive ion mode) and m/z 564-906 (negative ion mode). Guided by the H&E-stained cryosection slide, deposited matrix spots representing tumor-rich area were selected using FlexImaging software (version 2.1, Bruker Daltonics) for each tumor sample (Figure 1). Mass spectra data from selected spots was then exported to ClinProTools (version 2.2, Bruker Daltonics) for further data processing.

Data processing and statistical analysis

Baseline subtraction, spectral recalibration, and spectral area calculation were performed using ClinProTools (version 2.2, Bruker Daltonics). A resolution of 300 was applied to the peak detection method, and the Top Hat baseline with 10% minimal baseline width was used for baseline subtraction. Data reduction was performed at a factor of four, and spectra were recalibrated with a maximal peak shift of 2,000 ppm between reference and peak masses. All data with signal-to-noise ratios >5 were acquired. An average peak list was set up for each tissue sample by choosing peaks on the calculated total average spectrum for each tissue sample to create one average spectrum per patient. After excluding peak m/z 616 (non-lipid) in the positive mode, we normalized positive-mode datasets and negative-mode datasets to the average area. Average-normalized datasets (i.e., positive- and negative-mode lipid datasets) were then combined into a single dataset and subjected to statistical analysis using BRB-ArrayTools (NCI, USA, version 4.1) [13]. We performed class prediction analyses using all classifier functions of BRB-ArrayTools (compound covariate predictor, diagonal linear discriminant analysis, 1- and 3-nearest neighbors, nearest centroid, and support vector machine). Class prediction analyses were first performed by randomly dividing the training set into two (training and test) subsets at 1-to-1 ratio (i.e., 7 and 7 pairs).

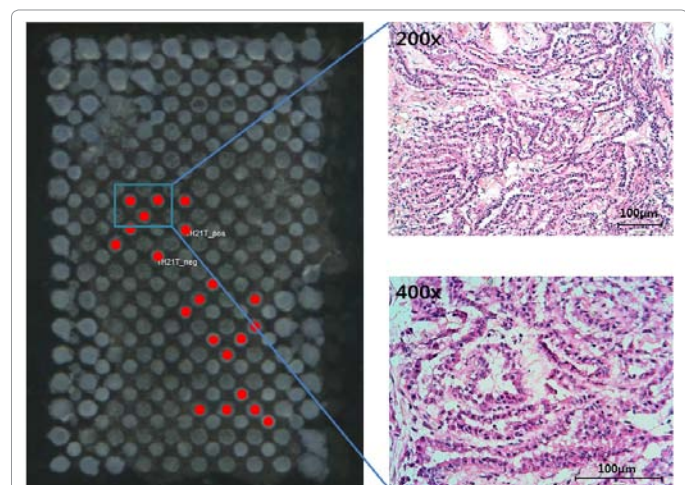


Figure 1: General procedure. Representative optical image of the cryosection ITO slide with matrix (left) and magnified areas of the H&E-stained consecutive cryosection slide of a tumor sample (right) are shown. The H&E-stained cryosection slide was evaluated for tumor-rich (>75%) area. Guided by the H&E-stained cryosection slide, deposited matrix spots on ITO cryosection slides representing tumor-rich area (shown in red) were selected using FlexImaging software for each tumor sample. Similar procedures were performed for normal tissue samples. Mass spectra data from selected spots was then exported to ClinProTools for further data processing.

	Training set	Validation set
Number of patients	14 (paired samples)	8 (unpaired samples)
Median age (year)	49.5	55
Gender		
Female	13 (93%)	7 (88%)
Male	1 (7%)	1 (12%)
Primary tumor location		
Unilateral	10 (71.4%)	8 (100%)
Bilateral	4 (28.6%)	0 (0%)
Surgery		
Total thyroidectomy	13 (93%)	8 (100%)
Lobectomy	1 (7%)	0 (0%)
Pathologic stage, AJCC¹		
Age < 45		
Stage I		
T1bN0	1 (7.1%)	0
T3N1a	3 (21.4%)	1 (50.0%)
Stage III		
Age ≥ 45		
Stage I		
T1aN0	2 (14.3%)	0
Stage III		
T3N0	4 (28.6%)	1 (50.0%)
T3N1a	4 (28.6%)	0

¹AJCC, American Joint Committee on Cancer (7th Edition)

Table 1: Patient characteristics.

nQuery Advisor software (version 7.0, Statistical Solutions, Saugus, MA) was used for randomization. Each classifier predicted class labels of 7 pairs in the test set for each of 100 random training-to-test partitions. Informative peaks identified in training set (14 pairs) were then used to predict class labels of 8 samples in the validation set.

MALDI LIFT (MS/MS) analysis was performed on cryosections after MALDI MS and the data were mapped to public lipid databases (www.lipidmaps.org).

Results

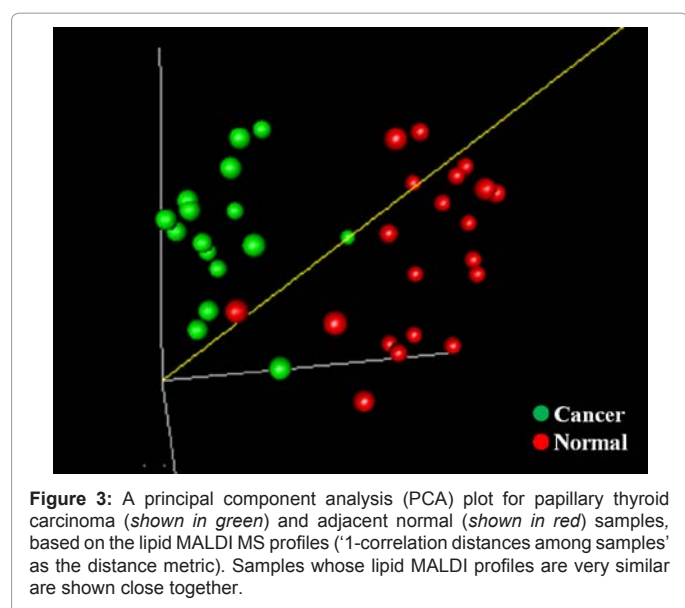
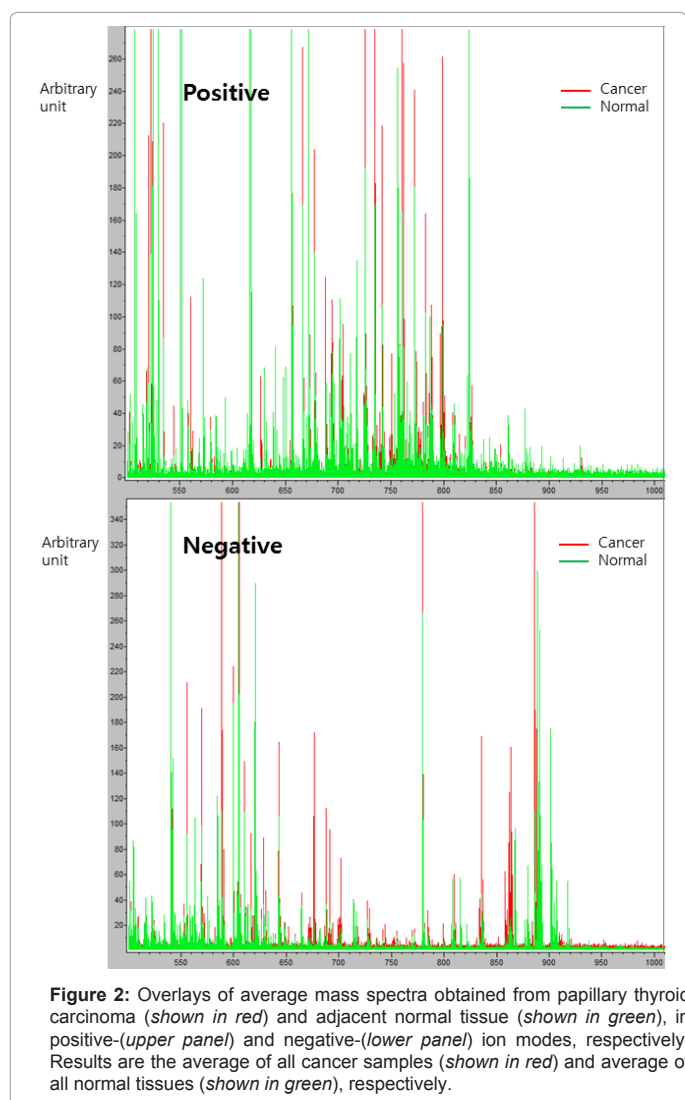
MALDI MS analyses were performed for 36 surgical tissue samples (16 cancers and 20 adjacent normal tissue samples) from 22 patients (Table 1). Among these 36 samples, 28 samples (14 tumor/normal pairs) were from the same patients. These 14 tumor/normal pairs were used as a training set. Another 8 unpaired samples (2 cancers and 6 adjacent normal tissue samples) were used as a validation set.

In the positive ion mode, MALDI MS signals from 3 to 20 spots (with a median value of 11) were averaged to generate an average mass spectrum for each cancer sample, and signals from 3 to 23 spots (with a median value of 15) were averaged in normal samples. In the negative ion mode, MALDI MS signals from 3 to 26 spots (with a median value of 13) were averaged to generate an average mass spectrum for each cancer sample, and signals from 5 to 19 spots (with a median value of 14) were averaged in normal samples. As shown in figure 2, 84 features (39 and 45 for positive and negative modes, respectively) were finally processed for subsequent analyses.

Papillary thyroid carcinomas in the training set demonstrated

significantly different lipid profiles from normal tissue samples. There were 27 lipid peaks differentially expressed between cancer and normal at a feature selection P value <0.001 , and the probability of getting at least 27 peaks significant by chance if there are no real differences between cancer and normal samples is less than 0.001, suggesting the clear difference in lipid profiles (Table 2). According to the principal component analysis, papillary thyroid carcinoma samples were separately clustered from adjacent normal tissue samples (Figure 3).

We performed class prediction analysis after randomly dividing 28 training set samples into two groups at 1-to-1 ratio. The median class prediction accuracy of all predictors in random test sets was 100% (7 out of 7 pairs) in 100 random training-to-test partitions (feature selection $P < 0.001$). Then, 8 additional samples (2 cancer and 6 adjacent normal samples) were used to validate informative peaks identified using 14 pairs of samples in the training set. Using peaks differentially expressed between 14 pairs of cancer and adjacent normal samples, we could correctly predict 100% of validation set samples (8 out of 8 samples) by all predictors. These results clearly demonstrate that papillary thyroid carcinomas and adjacent normal tissues have distinct lipid profiles (Supplementary table 1).



Seven tumor samples were collected from American Joint Committee on Cancer (AJCC) stage I thyroid cancer patients and 9 tumor samples were from stage III patients (Table 1). There were 3 peaks differentially expressed between cancer and normal at a feature selection P value <0.1 , and the probability of getting at least 3 peaks significant by chance if there are no real differences according to stage was 0.78. This result indicates that lipid profiles are not significantly different between stage I and stage III cancers.

Using MS/MS analysis, we identified lipid MALDI peaks differentially expressed between cancer and normal tissue samples at a feature selection P value <0.001 (Figure 4). Peaks m/z 741.6, m/z 772.7, and m/z 798.6 in the positive ion mode, that were overexpressed in thyroid cancer, were identified as sphingomyelin (SM) 34:1, phosphatidylcholine (PC) 32:0, and PC 34:1 (Figure 4A). Peaks m/z 599.5, m/z 835.6, m/z 861.7, and m/z 885.7 in the negative ion mode, that were overexpressed in thyroid cancer, were identified as phosphatidylinositol (PI) (18:0/0:0), PI (16:0/18:1), PI:Cer (d18:1/22:0) and PI (18:0/20:4) (Figures 4B and 4C). Lysophosphatidylcholine 18:3 (m/z 518.4 in the positive ion mode) and lysophosphatidylserine 18:1 (m/z 524.4 in the positive ion mode) were identified as lipids under expressed in papillary thyroid carcinomas (Figure 4D).

Discussion

This study demonstrates that the lipid profiles are different between papillary thyroid carcinoma and adjacent normal tissue samples. We identified phosphatidylcholines 32:0, and 34:1 as overexpressed peaks in papillary thyroid carcinoma. While we prepared this manuscript, Ishikawa et al. [12] reported that PC 32:0, PC 34:1 and SM 34:1 are overexpressed in a thyroid cancer patient. Our study extends the finding of prior smaller-scale lipid MALDI MS study, by assigning a larger number of cancer-associated peaks and by demonstrating the diagnostic utility of this approach in prospective clinical samples. Collectively, our data comprise an unparalleled comprehensive list of papillary thyroid carcinoma-specific lipids. Increase in the phosphatidylcholine content has been observed in several common solid tumors [8-10]. Since phosphatidylcholine is a major constituent of cell membrane, phosphatidylcholine requirement may increase

<i>Overexpressed in cancer</i>						
Peak	P	FDR	Normal	Cancer	Ratio ¹	Assignment
p741.6	0.0001	0.0008	8.1	12.0	1.5	SM (34:1) K+
p750.5	<0.0001	0.0002	7.8	14.6	1.9	
p772.7	<0.0001	0.0002	5.5	9.1	1.6	PC (32:0) K+
p798.6	0.0001	0.0005	7.5	14.5	1.9	PC (34:1) K+
n552.6	0.0006	0.0019	3.1	3.5	1.1	
n588.2	0.0001	0.0005	8.3	12.0	1.4	
n599.5	0.0001	0.0008	7.3	9.6	1.3	PI (18:0/0:0)
n616.6	0.0004	0.0016	2.4	3.3	1.4	
n687.6	0.0007	0.0023	5.8	7.5	1.3	
n701.7	<0.0001	0.0001	3.4	5.5	1.6	
n835.6	<0.0001	<0.0001	3.0	7.5	2.5	PI (16:0/18:1)
n857.7	<0.0001	<0.0001	1.4	2.7	2.0	
n861.7	<0.0001	<0.0001	1.8	4.4	2.4	PI-Cer (d18:1/22:0)
n885.7	<0.0001	0.0002	3.0	13.9	4.8	PI (18:0/20:4)
<i>Underexpressed in cancer</i>						
Peak	P	FDR	Normal	Cancer	Ratio ¹	Assignment
p518.4	0.0003	0.0015	1.7	1.2	0.7	LPC (18:3)
p524.4	0.0002	0.0012	2.2	3.5	0.4	LPS (18:1)
p572.3	0.0005	0.0017	2.2	1.1	0.5	
p650.5	0.0002	0.0009	3.0	2.0	0.7	
p672.1	0.0004	0.0016	3.6	1.5	0.4	
p701.6	0.0001	0.0008	2.6	1.3	0.5	
p705.5	<0.0001	0.0002	5.8	3.6	0.6	
p717.5	0.0008	0.0025	4.8	2.8	0.6	
n533.5	0.0004	0.0016	4.3	3.4	0.8	
n555.2	0.0003	0.0015	3.1	3.5	0.7	
n563.2	0.0005	0.0017	4.8	3.2	0.7	
n584.5	<0.0001	0.0003	14.5	6.3	0.4	
n620.2	0.0001	0.0008	11.5	6.4	0.6	

¹Ratio, Ratio of cancer to normal;

²p741.6, m/z 741.6 in the positive ion mode;

³n552.6, m/z 552.6 in the negative ion mode

FDR: False Discovery Rate; SM: Sphingomyelin; PC: Phosphatidylcholine; PI: Phosphatidylinositol; PI: Cer, Phosphatidylinositol:ceramide; LPC: Lysophosphatidylcholine; LPS: Lysophosphatidylserine

Table 2: Peak differentially expressed between papillary thyroid carcinoma and normal tissue at p<0.001.

in rapidly growing cells. Elyahu et al. [14] reported that choline transport rates and choline kinase activity increase by several fold in breast cancer, leading to increased phosphocholine. Increased phosphocholine, in turn, may contribute to the increased content of phosphatidylcholine in cancer. Several investigators reported that choline kinase plays a role in carcinogenesis [15-17]. Thus, increase in phosphatidylcholines 32:0, and 34:1 is consistent with the data in the literature. Our study also reveals that lysophosphatidylcholine 18:3 and lysophosphatidylserine 18:1 were underexpressed in papillary thyroid carcinomas, compared with normal tissue. While lysophospholipids are generated by phospholipase and reactive oxygen species generated in inflammatory conditions [18], decrease in these lysophospholipids

in cancers has not been reported thus far. Further studies are needed to validate this interesting finding.

Our study demonstrates that the lipid MALDI MS profiles distinguish cancerous epithelium from normal epithelium at 100% accuracy, for the first time to our knowledge. Papillary thyroid carcinomas often pose a diagnostic challenge to pathologists. In this regard, our finding that papillary thyroid carcinomas and normal tissue have highly distinct lipid profiles is noteworthy. In addition to the high classification power, potential advantages of histology-directed lipid MALDI MS analysis may include low reagent cost, rapid experimental procedure, and small amount of tissue required for the analysis. Hence, further studies using larger clinical sample sets may be warranted to

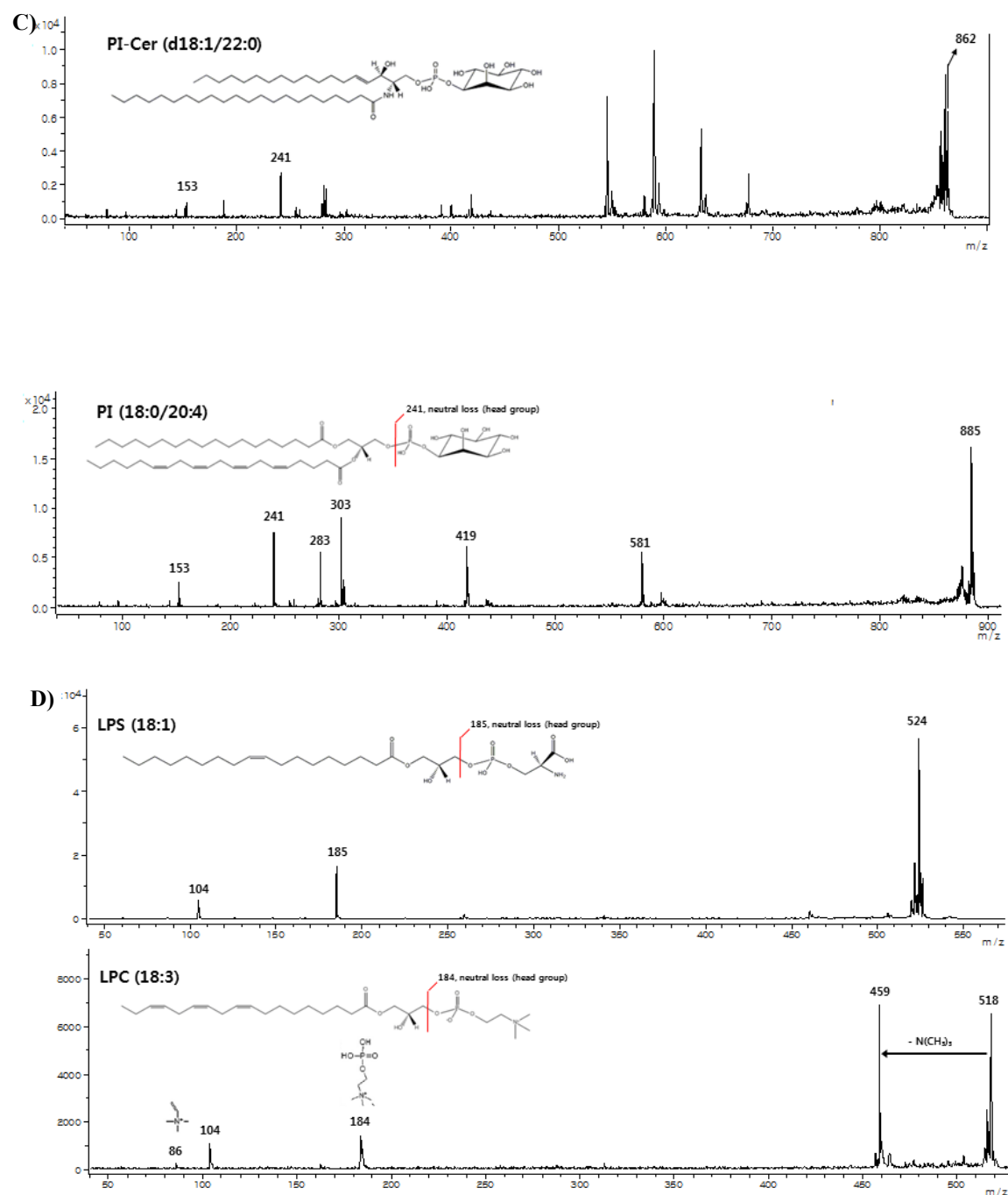


Figure 4: Molecular identification using MALDI LIFT (MS/MS) analyses. (A) Peaks at m/z 741.6, 772.7, and 798.6 in the positive ion mode (B) Peaks at m/z 599.5 and 835.6 in the negative ion mode (C) Peaks at m/z 861.7 and 885.7 in the negative ion mode (D) Peaks at m/z 518.4 and 524.4 in the positive ion mode.

evaluate the possibility of clinical translation of lipid profiles we have identified.

Acknowledgement

The work was supported by grants from Converging Research Center Program (2012K001506), through the Ministry of Education, Science and Technology of Korea and Proteogenomic Research Program through the National Research Foundation of Korea funded by the Korean Ministry of Education, Science and Technology.

References

1. Jung KW, Park S, Kong HJ, Won YJ, Lee JY, et al. (2012) Cancer statistics in Korea: incidence, mortality, survival, and prevalence in 2009. *Cancer Res Treat* 44: 11-24.
2. Cho BY, Choi H, Park YJ, Lim JA, Ahn HY, et al. (2013) Changes in the clinicopathological characteristics and outcomes of thyroid cancer in Korea over the past 4 decades. *Thyroid*.
3. Cibas ES, Sanchez MA (2008) The National Cancer Institute thyroid fine-

- needle aspiration state-of-the-science conference: inspiration for a uniform terminology linked to management guidelines. *Cancer* 114: 71-73.
4. Cibas ES, Ali SZ (2009) The Bethesda system for reporting thyroid cytopathology. *Thyroid* 19: 1159-1165.
 5. Renshaw AA (2002) Focal features of papillary carcinoma of the thyroid in fine-needle aspiration material are strongly associated with papillary carcinoma at resection. *Am J Clin Pathol* 118: 208-210.
 6. McHenry CR, Phitayakorn R (2010) Difficult problems in thyroid cancer surgery. *Minerva Chir* 65: 83-93.
 7. Kim HK, Reyzer ML, Choi IJ, Kim CG, Kim HS, et al. (2010) Gastric cancer-specific protein profile identified using endoscopic biopsy samples via MALDI mass spectrometry. *J Proteome Res* 9: 4123-4130.
 8. Lee GK, Lee HS, Park YS, Lee JH, Lee SC, et al. (2012) Lipid MALDI profile classifies non-small cell lung cancers according to the histologic type. *Lung Cancer* 76: 197-203.
 9. Kang HS, Lee SC, Park YS, Jeon YE, Lee JH, et al. (2011) Protein and lipid MALDI profiles classify breast cancers according to the intrinsic subtype. *BMC Cancer* 11: 465.
 10. Kang S, Lee A, Park YS, Lee SC, Park SY, et al. (2011) Alteration in lipid and protein profiles of ovarian cancer: similarity to breast cancer. *Int J Gyn Cancer* 21: 1566-1572.
 11. Thomas A, Patterson NH, Marcinkiewicz MM, Lazaris A, Metrakos P, et al. (2013) Histology-driven data mining of lipid signatures from multiple imaging mass spectrometry analyses: application to human colorectal cancer liver metastasis biopsies. *Anal Chem* 85: 2860-2866.
 12. Ishikawa S, Tateya I, Hayasaka T, Masaki N, Takizawa Y, et al. (2012) Increased expression of phosphatidylcholine (16:0/18:1) and (16:0/18:2) in thyroid papillary cancer. *PLoS One* 7: e48873.
 13. Simon R, Lam A, Li MC, Ngan M, Menenzes S, Zhao Y (2007) Analysis of gene expression data using BRB-ArrayTools. *Cancer Inform* 3: 11-17.
 14. Eliyahu G, Kreizman T, Degani H (2007) Phosphocholine as a biomarker of breast cancer: molecular and biochemical studies. *Int J Cancer* 120: 1721-1730.
 15. Bañez-Coronel M, Ramirez de Molina A, Rodriguez-Gonzalez A, Sarmentero J, et al. (2008) Choline kinase alpha depletion selectively kills tumoral cells. *Curr Cancer Drug Targets* 8: 709-719.
 16. Rodriguez-Gonzalez A, Ramirez de Molina A, Fernandez F, Lacal JC (2004) Choline kinase inhibition induces the increase in ceramides resulting in a highly specific and selective cytotoxic antitumoral strategy as a potential mechanism of action. *Oncogene* 23: 8247-8259.
 17. Glunde K, Raman V, Mori N, Bhujwalla ZM (2005) RNA interference-mediated choline kinase suppression in breast cancer cells induces differentiation and reduces proliferation. *Cancer Res* 65: 11034-11043.
 18. Fuchs B, Muller K, Paasch U, Schiller J (2012) Lysophospholipids: potential markers of diseases and infertility? *Mini Rev Med Chem* 12: 74-86.